Cluster radioactivity in extreme laser fields: A study for nuclear structure properties*

Leng-Jun Liao (廖堎君)[1] Xiao-Hua Li (李小华)[1,2,3,4,5†]

[1]School of Nuclear Science and Technology, University of South China, Hengyang 421001, China
[2]National Exemplary Base for International Sci & Tech. Collaboration of Nuclear Energy and Nuclear Safety, University of South China, Hengyang 421001, China
[3]Cooperative Innovation Center for Nuclear Fuel Cycle Technology & Equipment, University of South China, Hengyang 421001, China
[4]Key Laboratory of Low Dimensional Quantum Structures and Quantum Control, Hunan Normal University, Changsha 410081, China
[5]Key Laboratory of Advanced Nuclear Energy Design and Safety, Ministry of Education, Hengyang 421001, China

Abstract: In the present work, we investigate the effect of ultra-intense laser fields on cluster radioactivity from a nuclear-structure perspective. Specifically, we examine the relationship between the maximum instantaneous rate of change of the penetration probability and the proton number of the emitted cluster. Subsequently, based on the characteristics of cluster-radioactive nuclei, we investigate the correlation between the rate of change of the penetration probability and the neutron number of the daughter nuclei for the emission of ^{14}C from Ra, ^{20}O from Th, ^{23}F from Pa, ^{24}Ne from U, ^{28}Mg from Pu, and ^{34}Si from Cm isotopes. The results demonstrate that shell effects contribute to the rate of change of the penetration probability. Notably, the influence of the neutron shell effect on this rate diminishes as the number of valence protons increases. In addition, the rate of change exhibits an overall linear increase with the quadrupole deformation parameter of the parent nucleus. Finally, the effect of odd-even staggering on laser-assisted cluster radioactivity is revealed. This research provides valuable insights for future laser-nuclear physics experiments.

Keywords: cluster radioactivity, ultra-intense laser field, penetration probability, odd-even staggering, shell effect

DOI: 10.1088/1674-1137/ae84aa **CSTR:** 32044.14.ChinesePhysicsC.50104103

I. INTRODUCTION

The field of nuclear physics originated with Henri Becquerel's seminal discovery of natural radioactivity in 1896. Since then, scientists have experimentally observed various radioactive decay modes, among which alpha decay and spontaneous fission are the two primary modes for heavy and superheavy unstable nuclei [1]. Bridging these two regimes is a unique phenomenon known as cluster radioactivity. This process involves the spontaneous emission, from an unstable heavy or superheavy nucleus, of a cluster particle that is heavier than an α particle but lighter than the fragments produced in spontaneous fission. This exotic radioactive decay mode was first theoretically proposed by Sandulescu *et al.* in 1980 based on the Super-Asymmetric Fission Model (SAFM) [2]. It was subsequently confirmed experimentally by Rose *et al.* in 1984 [3], after which it rapidly became an active research area in nuclear physics [4−13].

In recent years, breakthroughs in high-intensity laser technology have opened entirely new avenues for the study of cluster radioactivity [14−17]. For instance, driven by the chirped-pulse amplification (CPA) technique, peak laser intensity has reached 10^{23} W/cm^2 [16]. Concurrently, X-ray Free Electron Lasers (XFELs) can now generate coherent light with photon energies up to 20 keV, thereby covering the low-lying excited states of some atomic nuclei [17]. Research on laser-assisted cluster radioactivity is important, largely because of its potential application in the purification of radioactive nuclear waste.

For cluster radioactive nuclides in the trans-lead re-

Received 28 February 2026; Accepted 29 June 2026; Accepted manuscript online 30 June 2026

* This work is supported in part by the National Natural Science Foundation of China (12175100, 11975132), the construct program of the key discipline in Hunan Province, the Research Foundation of Education Bureau of Hunan Province, China (18A237, 22A0305, 19A440), the Shandong Province Natural Science Foundation, China (ZR2022JQ04), the Opening Project of Cooperative Innovation Center for Nuclear Fuel Cycle Technology and Equipment, University of South China (2019KFZ10), the Innovation Group of Nuclear and Particle Physics in USC, Hunan Provincial Innovation Foundation for Postgraduate (CX20251453). Science and technology plan project of Hengyang city (202150063428). Key Laboratory of Advanced Nuclear Energy Design and Safety, Ministry of Education(KLANETDS -KF-202414)

† E-mail: lixiaohuaphysics@126.com

gion, the daughter nuclei are typically the doubly magic nucleus ^{208}Pb and its neighboring nuclei [18−20]. The dominance of the doubly magic structure in heavier fragments reveals the influence of shell effects on cluster radioactivity. Given the correlation between the *n*-*p* interaction and shell effects [8], this suggests a dependence of cluster radioactivity on the *n*-*p* interaction. Furthermore, nucleon pairing correlations induce odd-even staggering, which significantly affects cluster radioactivity [21]. Therefore, an in-depth exploration of the influence of nuclear structure information, such as shell effects, the *n*-*p* interaction, and odd-even staggering, on laser-assisted cluster radioactivity is important for understanding laser-nuclear interactions. Moreover, this provides a new perspective for future experiments in laser-nuclear physics.

In this work, we present a quantitative investigation of how extreme laser fields affect the penetration probability of cluster radioactivity. Nuclear deformation is incorporated to ensure accuracy, as the electric dipole term depends on the angle between the direction of the laser field and that of cluster emission. The results indicate that extreme laser fields attainable in the near future can slightly modify the penetration probability of cluster radioactivity. We then discuss in detail the effects of shell effects and parity staggering on the maximum instantaneous rate of change of the penetration probability. Notably, we reveal that the neutron shell effect on this rate gradually weakens as the number of valence protons increases. Additionally, the overall rate of change exhibits a linear increase with the quadrupole deformation parameter of the parent nucleus. Finally, we examine the correlation between the rate of change of the penetration probability and the decay energy for various parent nuclei emitting the same cluster. We find that shell effects play a significant role, manifesting as two distinct inverse trends with different slopes.

This paper is organized as follows. The theoretical framework for calculating the cluster radioactivity half-life in extreme laser fields and the laser-nucleus interaction are presented in Sec. II. Detailed calculation results and discussion are provided in Sec. III. A brief summary is given in Sec. IV.

II. THEORETICAL FRAMEWORK

The half-life of cluster radioactivity is expressed as [22]

$$T_{1/2} = \frac{\ln 2}{\lambda}, \tag{1}$$

where λ is the decay constant for cluster emission, which depends on the assault frequency ν, the penetration probability P, and the cluster radioactivity preformation probability P_c. It is given by the following equation [23],

$$\lambda = \nu P P_c. \tag{2}$$

Here, the cluster preformation probability P_c is calculated using an empirical formula proposed by Santhosh *et al.* [22], and it can be written as

$$P_c = 10^{aZ_cZ_d+b}, \tag{3}$$

where Z_c and Z_d represent the proton numbers of the emitted cluster and daughter nucleus, respectively. The adjustable parameters a=−0.01555 and b=3.22940 are taken from Ref. [24]. $\nu = \frac{\omega}{2\pi} = \frac{2E_\nu}{\hbar}$ in Eq. (2) denotes the number of collective assaults per unit time by the emitted cluster on the potential barrier. $\hbar$ denotes the reduced Planck constant. E_ν is the vibrational energy of the emitted cluster inside the barrier, which is evaluated using the following semi-empirical formula [25],

$$E_\nu = Q_c\{0.056 + 0.039\exp(\frac{4-A_c}{2.5})\} \qquad \text{for } A \geqslant 4. \tag{4}$$

Here, A_c and A denote the mass numbers of the emitted cluster and the parent nucleus, respectively. Q_c is the decay energy associated with cluster radioactivity and can be expressed as

$$Q_c = B(A_c,Z_c) + B(A_d,Z_d) - B(A,Z), \tag{5}$$

where $B(A_c,Z_c)$, $B(A_d,Z_d)$, and $B(A,Z)$ are the binding energies of the emitted cluster, daughter nucleus, and parent nucleus, respectively. They are taken from AME2020 [26] and NUBASE2020 [27]. A_d and Z are, respectively, the mass number of the daughter nucleus and the proton number of the parent nucleus.

Since the daughter nucleus in cluster radioactivity is usually the doubly magic nucleus ^{208}Pb or a nucleus near it, and thus exhibits a spherical or near-spherical shape [28], we consider only the effect of the deformation of the emitted cluster in the present work. The total penetration probability P is obtained by averaging P_φ over all directions. They are given as [24]

$$P = \frac{1}{2}\int_0^\pi P_\varphi \sin\varphi \mathrm{d}\varphi, \tag{6}$$

$$P_\varphi = \exp\left[-\frac{2\sqrt{2\mu}}{\hbar}\int_{\mathrm{R_{in}}}^{\mathrm{R_{out}}} \sqrt{V(r,\varphi,t,\theta) - Q_c}\mathrm{d}r\right], \tag{7}$$

where φ is the orientation angle of the symmetry axis of the deformed cluster. θ is the angle between the vector $\boldsymbol{r}$ and the vector $\boldsymbol{\varepsilon}(t)$. $\boldsymbol{r}$ is the vector between the centers of the emitted cluster and the daughter nucleus. $\varepsilon(t)$ is related to the laser-nucleus interaction, which will be described in more detail below. $\mu = \dfrac{M_d M_c}{M_d + M_c}$ represents the reduced mass of the emitted cluster-daughter nucleus system, with M_c and M_d being the masses of the emitted cluster and daughter nucleus, respectively. $R_{\rm in} = C_c + C_d$ [29] is the saddle point for the touching configuration, with $C_i = R_i\left(1-\dfrac{b^2}{R_i^2}\right)$ $(i = c,d)$ being the Süssmanncentral radii [30] of the daughter nucleus and the emittedcluster. The diffuseness parameter of the nuclear surface, $b = 1$ fm, is taken from Ref. [31]. The sharp radius R_i can be defined as [32]

$$R_i = 1.28A_i^{1/3} - 0.76 + 0.8A_i^{-1/3}. \tag{8}$$

$R_{\rm out}$ in Eq. (7) is the outer turning point of the barrier, determined by the condition $V(r,\varphi,t,\theta) = Q_c$[33]. Here, $V(r,\varphi,t,\theta)$ denotes the total interaction potential between the emitted cluster and the daughter nucleus. It can be written as

$$V(r,\varphi,t,\theta) = V_N(r,\varphi) + V_C(r,\varphi) + V_l(r) + V_I(r,t,\theta), \tag{9}$$

where $V_N(r,\varphi)$, $V_C(r,\varphi)$, and $V_l(r)$ denote the nuclear, Coulomb, and centrifugal potentials, respectively. $V_I(r,t,\theta)$ represents the interaction of the laser field with the decay system, and a more detailed description of this interaction is provided below.

In this work, the nuclear potential $V_N(r,\varphi)$ is chosen in the conventional Woods-Saxon form [34], accounting for the axially symmetric deformation of the emitted cluster, and is given as

$$V_N(r,\varphi) = \frac{V_0}{1+\exp\left[\dfrac{r-R(\varphi)}{a}\right]}, \tag{10}$$

with

$$R(\varphi) = -1.37 + r_d + r_c\left[1+\beta_2 Y_{20}(\varphi) + \beta_4 Y_{40}(\varphi) + \beta_6 Y_{60}(\varphi)\right]. \tag{11}$$

Here, β_2, β_4, and β_6 correspond to the quadrupole, hexadecapole, and hexacontatetrapole deformation coefficients of the emitted cluster, respectively. They are obtained from FRDM2012 [35]. $Y_{lm}(\varphi)$ is the spherical harmonics function. $r_i = 1.27A_i^{1/3}$ $(i = c,d)$ denotes the nuclear charge radii. The potential depth V_0 and diffuseness a are parameterized as [34]

$$V_0 = -44.16[1-0.4(I_d+I_c)]\frac{A_d^{1/3}A_c^{1/3}}{A_d^{1/3}+A_c^{1/3}}, \tag{12}$$

$$a = 0.5 + 0.33I_d, \tag{13}$$

where $I_i = \dfrac{N_i - Z_i}{A_i}$ $(i = c,d)$ denotes the relative neutron excess of the emitted cluster or daughter nucleus, and N_i $(i = c,d)$ is the neutron number of the corresponding nucleus.

The deformed Coulomb potential $V_C(r,\varphi)$ in Eq. (9) is given by [36, 37]

$$V_C(r,\varphi) = \frac{Z_c Z_d e^2}{r} + 3Z_c Z_d e^2 \sum_\lambda \frac{1}{2\lambda+1} \times \frac{R^\lambda(\varphi)}{r^{\lambda+1}} Y_{\lambda 0}(\varphi)\left[\beta_\lambda + \frac{4}{7}\beta_\lambda^2 Y_{\lambda 0}(\varphi)\right]. \tag{14}$$

The centrifugal potential $V_l(r)$ is expressed in the Langer-modified form, since the replacement $l(l+1) \to (l+1/2)^2$ is a necessary correction for one-dimensional problems [23]. It can be written as

$$V_l(r) = \frac{\hbar^2 (l+\frac{1}{2})^2}{2\mu r^2}. \tag{15}$$

Here, l denotes the orbital angular momentum carried by the emitted cluster, and its value is determined from the spin-parity conservation rule, which can be expressed as [38]

$$l = \begin{cases} \triangle_j & \text{for even } \triangle_j \text{ and } \pi = \pi_d, \\ \triangle_j + 1 & \text{for even } \triangle_j \text{ and } \pi \neq \pi_d, \\ \triangle_j & \text{for odd } \triangle_j \text{ and } \pi \neq \pi_d, \\ \triangle_j + 1 & \text{for odd } \triangle_j \text{ and } \pi = \pi_d, \end{cases} \tag{16}$$

where $\triangle_j = |j - j_d - j_c|$. j, π, j_d, π_d, j_c, and π_c denote the spin and parity values of the parent nucleus, daughter nucleus, and emitted cluster, respectively. These values are taken from NUBASE2020 [27].

Since the emitted cluster, with a kinetic energy of only tens of MeV, moves much more slowly than light in vacuum, the laser electric field has a stronger influence on the emitted cluster than the laser magnetic field. Thus, the magnetic component of the laser field can be neglected. Therefore, this work considers only the influence of the laser electric field. The effect of the laser field on the nucleus is determined by the electric-dipole term, which can be written as

$$V_I(r,t,\theta) = -Z_{\rm eff}\boldsymbol{r}\cdot\boldsymbol{\varepsilon}(t) = -Z_{\rm eff}r\varepsilon(t)\cos\theta, \tag{17}$$

where $Z_{\rm eff} = (Z_cA_d - Z_dA_c)/A$ is the effective charge for relative motion. This effective charge describes the tendency of the laser electric field to separate the emitted cluster from the daughter nucleus[39]. The laser electric field $\varepsilon(t)$ is chosen to be a linearly polarized Gaussian plane wave. It can be given by [39]

$$\varepsilon(t) = \varepsilon_0 f(t)\sin(\omega t). \tag{18}$$

Here, ω represents the angular frequency. ε_0[MV·fm^{-1}] = 27.44× 10^{-19}(I_0 [W· cm^{-2}])$^{1/2}$ is the peak laser electric field, which is related to the peak laser intensity I_0 [40]. $f(t) = \exp(-t^2/\tau^2)$ describes the temporal profile of the Gaussian pulse envelope. $\tau = xT_0$ is the pulse width of the envelope, with T_0 denoting the pulse period.

In the context of the interaction between laser electric fields and cluster radioactivity, it is appropriate to consider the effect of the laser electric field on the decay energy. Thus, the decay energy, accounting for the influence of the laser electric field, can be expressed as

$$Q_c^* = Q_c + \Delta Q_c. \tag{19}$$

The change in decay energy ΔQ_c, which is equal to the energy gained by the emitted cluster as it is accelerated by the laser electric field while penetrating the barrier, can be defined as

$$\Delta Q_c = eZ_c\varepsilon(t)R(\varphi)\cos\theta. \tag{20}$$

Before proceeding further, it is necessary to briefly outline the limitations of the current theoretical framework. First, regarding nuclear deformation, the present model considers only the deformation of the emitted cluster while assuming the daughter nucleus to be spherical. Although this approximation is physically reasonable for trans-lead cluster radioactivity, where the daughter nuclei are typically the doubly magic nucleus ^{208}Pb or its neighbors, it limits the model's applicability to decay systems in which the daughter nucleus exhibits significant quadrupole or higher-order deformation. Second, the laser–nucleus interaction is strictly confined to the electric dipole approximation, neglecting higher-order multipole effects and magnetic contributions. Because the emitted clusters are non-relativistic and the long-wavelength condition holds, these neglected terms contribute minimally under the laser parameters studied here. However, if the model were extrapolated to relativistic cluster emission or extremely short-wavelength laser fields, such as hard X-ray or gamma-ray lasers, higher-order multipole and magnetic effects would become non-negligible, and the current model would no longer be valid. Finally, to evaluate the maximum possible impact of the laser field, we fixed the angle θ between the laser electric field and the cluster emission direction at 0. The current results therefore represent an upper limit of the laser's impact and do not reflect the statistical averaging that would arise from the random relative orientation between the laser and the nucleus in realistic experiments. Under a more realistic statistical distribution, the macroscopically observed rate of change in the penetration probability would be smaller than the maximum instantaneous value calculated in this work.

III. RESULTS AND DISCUSSION

In light of the anticipated availability of high-intensity laser pulses at ELI-NP and SULF in the coming years, we systematically investigate the effects of laser pulses with a peak intensity of $I_0 = 10^{24}$ W/cm^2 on cluster radioactivity. To ensure accuracy, we first discuss the feasibility of the adopted model. In this work, we calculate the cluster radioactivity half-lives of 26 trans-lead nuclei for which experimental data are available. The experimental data on cluster radioactivity half-lives are taken from Refs. [4, 8, 24, 34]. To provide an intuitive comparison between the calculated and experimental half-lives, we present these data in Fig. 1 (a). Moreover, the differences between the theoretical and experimental cluster radioactivity half-lives are shown in Fig. 1 (b). As shown in these figures, the theoretical half-lives obtained using our model are in good agreement with the experimental data, and the deviations are mainly within $-1 \to 1$. To obtain a quantitative measure of the deviation, the root-mean-square deviation σ is used. It can be expressed as

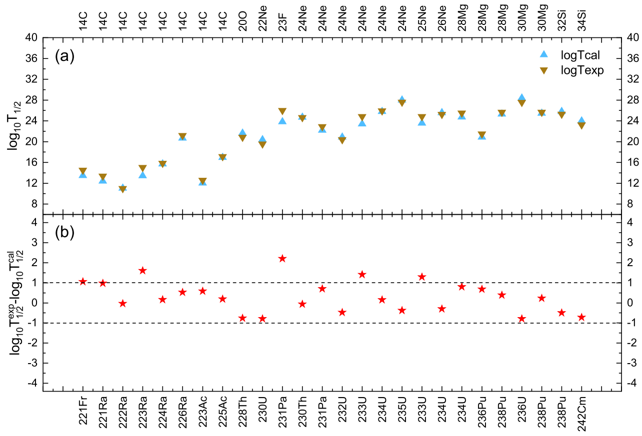

Fig. 1. (color online) (a) Comparison between the experimental cluster radioactivity half-lives and calculated ones. (b) The differences between the experimental and theoretical logarithmic half-lives.

$$\sigma = \sqrt{\frac{1}{n}\sum_{i=1}^{n}(\log_{10}T_{1/2}^{\mathrm{cal}.i} - \log_{10}T_{1/2}^{\mathrm{exp}.i})^2}, \tag{21}$$

where $\log_{10}T_{1/2}^{\mathrm{cal}.i}$ and $\log_{10}T_{1/2}^{\mathrm{exp}.i}$ denote the logarithmic forms of the theoretical and experimental half-lives for the i-th nucleus, respectively. n is the number of nuclei involved in the different cases. Using Eq. (21), we obtain a root-mean-square deviation of $\sigma = 0.848$. This indicates that our theoretical model is reliable.

Subsequently, to quantify the impact of the laser electric field on the cluster-radioactivity half-life for a fixed electric-field strength or at a given moment t, we define the relative change rate of the cluster-radioactivity half-life, denoted by ΔT. It can be written as

$$\Delta T = \frac{T(\varepsilon,\theta) - T(\varepsilon=0,\theta)}{T(\varepsilon=0,\theta)}. \tag{22}$$

Because the collision between the emitted cluster and the barrier occurs within the nucleus, the assault frequency ν is almost unaffected by external laser fields [41]. From Eqs. (1) and (2), it can be deduced that the effect of laser electric fields on the half-life of cluster radioactivity is manifested through changes in the cluster radioactivity penetration probability. The rate of change in the cluster radioactivity penetration probability is defined as

$$\Delta P = \frac{P(\varepsilon,\theta) - P(\varepsilon=0,\theta)}{P(\varepsilon=0,\theta)}. \tag{23}$$

Due to the direct equivalence between ΔP and ΔT, the subsequent discussion focuses exclusively on ΔP. In this study, using the adopted model, we systematically calculate the maximum instantaneous rate of change of the cluster radioactivity penetration probability, ΔP, for 26 trans-lead nuclei. The results are plotted in Fig. 2. In this figure, the horizontal axis represents the proton number of the emitted cluster. As shown, when $\theta = 0$, a laser electric field with an intensity of 10^{24} W/cm^2 causes a slight change in the penetration probability. In addition, the range of ΔP values for a given cluster emitted by different parent nuclei varies substantially. This range shifts approximately linearly toward higher values as the proton number of the emitted cluster increases. This phenomenon occurs because, when the radius vector $\vec{r}$ is aligned with the external field, an increase in the proton number Z_c of the emitted cluster increases the energy ΔQ_c gained from acceleration by the laser electric field during barrier penetration. This increase in ΔQ_c consequently leads to an increase in ΔP.

For cluster radioactive nuclides in the trans-lead region, the daughter nuclei are typically the doubly magic nucleus ^{208}Pb and its neighboring nuclei [18−20]. The

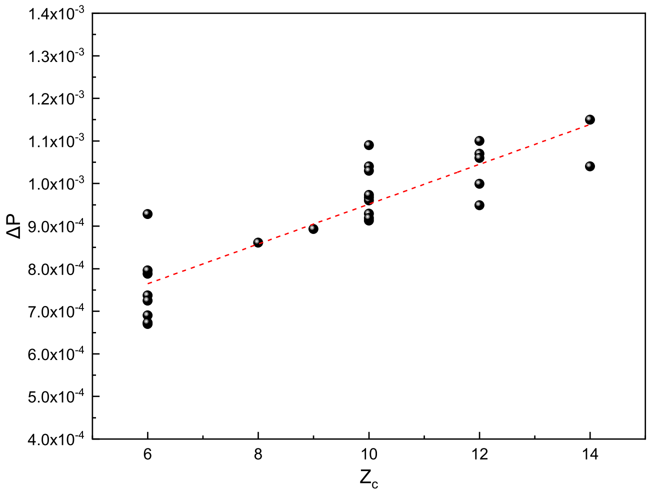

Fig. 2. (color online) The maximum instantaneous change rate of penetration probability for different parent nuclei for laser intensity of 10^{24} W/cm^2.

predominance of the doubly magic structure in heavier fragments reveals the influence of shell effects on cluster radioactivity. Furthermore, our previous work [42] indicated that, for different emitted clusters, the logarithmic form of the cluster radioactivity penetration probability increases linearly with the neutron number N_d of the daughter nuclei, reaches a maximum at $N_d = 126$, and then decreases linearly. This motivated us to investigate whether the shell effect observed in the penetration probability is also reflected in its rate of change under extreme laser-field conditions. In the present work, we select the following six isotopic chains to investigate the impact of shell effects on ΔP: the emission of ^{14}C from Ra, ^{20}O from Th, ^{23}F from Pa, ^{24}Ne from U, ^{28}Mg from Pu, and ^{34}Si from Cm isotopes. Fig. 3 illustrates the relationship between the maximum instantaneous rate of change of the penetration probability and the neutron number of the corresponding daughter nucleus. As shown, ΔP for all six chains exhibits a similar trend. For the emission of ^{14}C from Ra, ^{20}O from Th, ^{23}F from Pa, and ^{34}Si from Cm isotopes, the minimum ΔP occurs when the daughter nucleus is the doubly magic ^{208}Pb. Similarly, for the emission of ^{24}Ne from U isotopes and ^{28}Mg from Pu isotopes, the minimum value of ΔP occurs in the cluster radioactive process with the near doubly magic daughter nucleus ^{207}Pb. The low values of ΔP at $N_d = 126$ indicate the role of neutron magicity. This reveals that the nuclear shell structure effect is reflected in the rate of change of the penetration probability, and the role of neutron shell closure in laser-assisted cluster radioactivity is more crucial than that of proton shell closure. Consequently, future experiments should employ decays far from doubly magic daughter nuclei to achieve a more significant rate of change in the cluster radioactivity penetration probability.

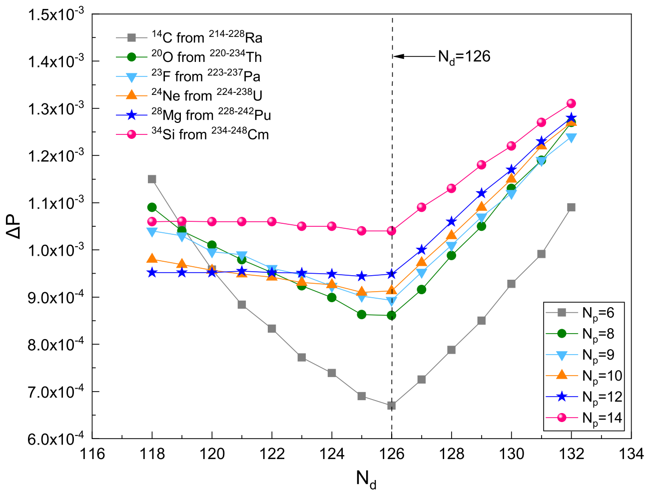

Fig. 3. (color online) Impact of the shell effect on ΔP for the emission of clusters ^{14}C, ^{20}O, ^{23}F, ^{24}Ne, ^{28}Mg and ^{34}Si respectively from Ra, Th, Pa, U, Pu and Cm isotopes in the case of $I_0 = 10^{24}$ W/cm^2.

Recently, Wang *et al.* reported that, for nuclei with more valence protons (or neutrons), the influence of neutron (or proton) shell effects on the α decay process appears to weaken [43]. Since α decay and cluster radioactivity are governed by the same physical mechanism, it is worthwhile to investigate whether the influence of shell effects on the change rate of the cluster radioactivity penetration probability also depends on the number of valence protons (holes). As established earlier, the impact of extreme laser fields on the cluster penetration probability is significantly modulated by shell effects. To explore how valence protons (holes) affect this modulation, Fig. 3 illustrates the relationship between ΔP and the daughter neutron number for different numbers of valence protons (holes). The figure shows that, as the number of valence protons (holes) increases, the variation of ΔP with the daughter neutron number becomes more gradual. In other words, the neutron shell effect on ΔP progressively weakens as the number of valence protons (holes) increases. This implies that parent nuclei with more valence protons (holes) are more sensitive to the influence of laser fields.

Given the correlation between the number of valence nucleons (holes) and the ground-state shape of the nucleus, this result suggests a potential dependence of laser-assisted cluster radioactivity on nuclear ground-state shape. Closed-shell nuclei are generally spherical, whereas open-shell nuclei deform because of the polarization effect of valence nucleons (holes) on the core [44]. When the number of valence nucleons (holes) is small, the polarization effect is weak, and the nuclear ground-state shape deviates only slightly from a sphere. As the number of valence nucleons (holes) increases, the polarization effect strengthens, and the degree of nuclear deformation increases significantly. Combined with the previously established relationship between valence nucleons (holes) and the laser-induced influence on cluster radioactivity, this phenomenon motivates our investigation into whether laser-assisted cluster radioactivity depends on the degree of nuclear deformation. To verify this, we plot the correlation between ΔP and the quadrupole deformation of the parent nucleus in Fig. 4. The horizontal axis represents the quadrupole deformation coefficient of the parent nucleus. As shown in this figure, ΔP generally exhibits a linear increasing trend as the quadrupole deformation coefficient of the parent nucleus increases. This indicates that the effect of extreme laser fields on the penetration probability is influenced by the degree of nuclear deformation.

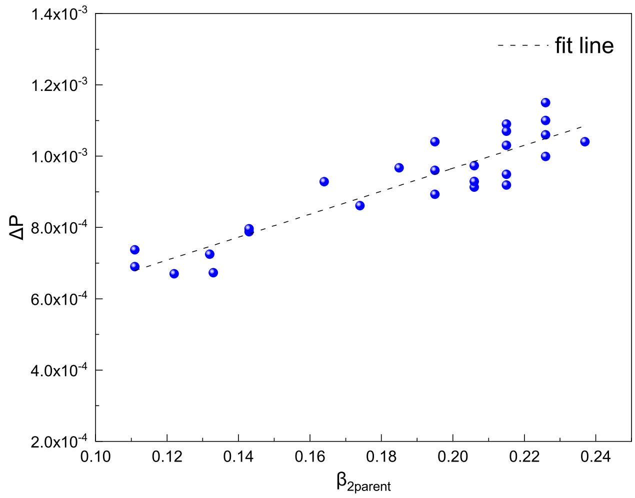

Fig. 4. (color online) The correlation between the relative change rate of cluster radioactivity penetration probability and quadrupole deformation of parent nucleus.

On the other hand, extensive researchers have established the significant influence of the odd-even staggering effect on cluster radioactivity [21, 23]. This effect is typically attributed to nucleonic pairing correlations [21]. It manifests as a sharp change in binding energy when transitioning from an even-N or even-Z nucleus to its odd-nucleon neighbor [23]. We hypothesize that the odd-even staggering effect may also influence the rate of change of the penetration probability under extreme laser field conditions. To validate this hypothesis, we select four isotope chains that emit clusters with different odd-even parities: the emission of ^{14}C from Ra, ^{23}F from Pa, and ^{24}Ne and ^{25}Ne from U isotopes. Fig. 5 illustrates the dependence of the rate of change of their penetration probability on the neutron number of the daughter nucleus under the influence of an extreme laser field. As shown in Fig. 5, for the emission of the ^{25}Ne cluster from uranium isotopes, ΔP increases when N_d changes from an even value to the next odd value and then decreases as N_d

changes to the next even value. This phenomenon suggests that the influence of laser fields on the penetration probability of cluster radioactivity is affected by nucleonic pairing correlations. Additionally, we find that the odd-even staggering effect is manifested only in the emission of clusters with an odd neutron number. This also indicates that neutron pairing plays a more dominant role than proton pairing in laser-assisted cluster radioactivity.

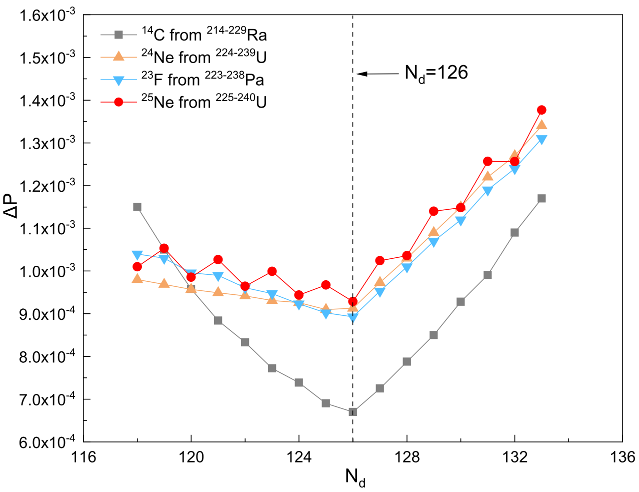

Fig. 5. (color online) Impact of the odd-even staggering effect on ΔP for the emission of clusters ^{14}C, ^{23}F, ^{24}Ne and ^{25}Ne respectively from Ra, Pa and U isotopes in the case of $I_0 = 10^{24}$ W/cm^2.

In our previous work, we found that, for different cluster-radioactive nuclei, the values of ΔP for emissions involving clusters with the same number of protons are negatively correlated with the decay energy Q_c [45]. To further examine this relationship, we plot the correlation between Q_c and ΔP for the cluster emissions of ^{14}C from Ra, ^{23}F from Pa, and ^{24}Ne and ^{25}Ne from U isotopes in Fig. 6. Although a general negative correlation persists across different cluster emissions, the relationship for a specific cluster is not simply linear. As shown in Fig. 6 (a), for the emission of the ^{24}Ne cluster from U isotopes, when N_d is less than 125 (near the neutron magic number 126), ΔP is inversely proportional to Q_c; when N_d is greater than 125, the two still exhibit inverse proportionality, but with a different slope. Similarly, as depicted in Fig. 6 (b), for the emission of ^{14}C from Ra, ^{23}F from Pa, and ^{25}Ne from U isotopes, when N_d is less than 126, ΔP and Q_c exhibit an inverse relationship; when N_d is greater than 126, the two show an inverse relationship with a different slope. This suggests that the relationship between ΔP and Q_c is influenced by the shell effect. Moreover, ΔP is more sensitive to changes in Q_c when N_d exceeds 126. This is because, when the number of neutrons in the daughter nucleus approaches or equals the magic number, the neutrons form a complete shell structure and have higher stability. However, when the number exceeds the magic number, the additional neutrons are located outside the stable shell and are more susceptible to the influence of the laser fields. Furthermore, based on the correlation between ΔP and Q_c, we can infer that the odd-even staggering reflected in the maximum instantaneous change rate of the penetration probability may also be observed in the decay energy Q_c. To verify this conjecture, we depict ΔP and Q_c for the cluster emission of ^{25}Ne from U isotopes in Fig. 7. This figure clearly shows that the decay energy is also affected by odd-even staggering, and its trend is opposite to that observed in the rate of change of the penetration probability.

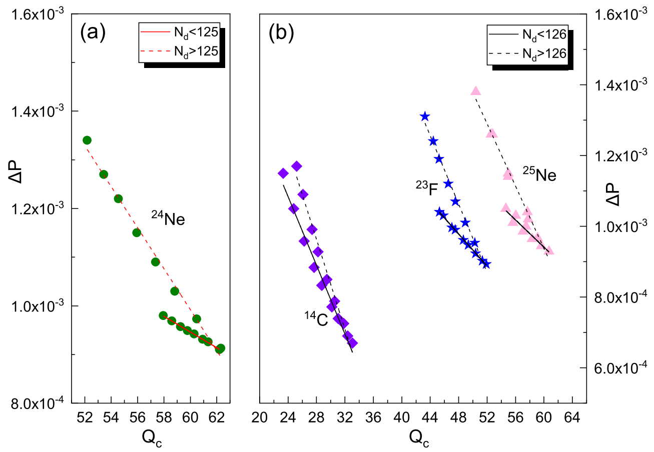

Fig. 6. (color online) Correlation between ΔP and Q_c for the emission of cluster ^{14}C from Ra isotopes, the emission of cluster ^{23}F from Pa isotopes, and the emission of clusters ^{24}Ne and ^{25}Ne from U isotopes in the case of $I_0 = 10^{24}$ W/cm^2. The two distinct inverse-slope regimes demarcated by the neutron magic number $N_d = 126$ and the neutron number $N_d = 125$ are clearly depicted.

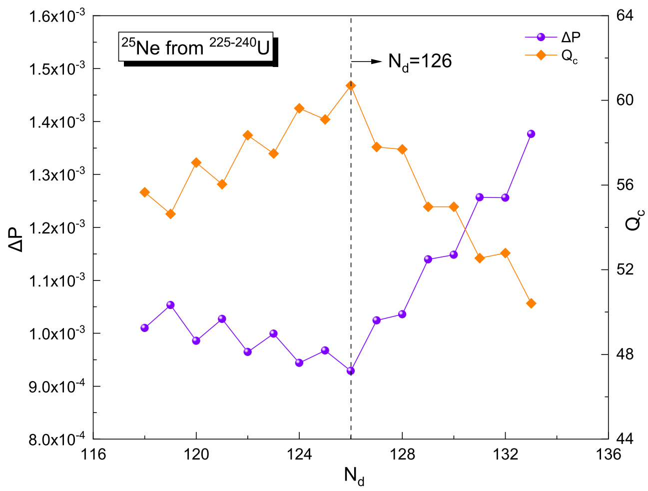

Fig. 7. (color online) Odd-even staggering of Q_c for the emission of cluster ^{25}Ne from U isotopes in the case of $I_0 = 10^{24}$ W/cm^2.

Before concluding, it is important to address the experimental feasibility of observing the predicted effects. The intensity of 10^{24} W/cm^2 considered in this work lies at the absolute frontier of near-future facilities like ELI-NP and SULF, which would require focusing a ~ 10 PW laser pulse to a near-diffraction-limited spot of ~ 1-2 μm with a duration of ~ 20-30 fs. At such extreme intensities, competing processes such as rapid ionization and plasma formation will inevitably occur in solid targets, leading to plasma shielding and Coulomb explosions that could preclude a clean observation of the laser-nucleus interaction. To mitigate these effects, future experiments might need to employ low-density targets such as gas jets or nanoclusters, or alternatively, utilize XFELs which can penetrate the plasma and couple directly to the nucleus. Furthermore, since the change rate ΔP scales approximately with $\sqrt{I_0}$, lower but more accessible intensities of 10^{22}-10^{23} W/cm^2 are expected to produce a ΔP on the order of 10^{-4} to 3×10^{-4}. Although measuring such a minute change in the penetration probability poses a significant challenge for current nuclear detection techniques, these theoretical predictions serve as an important benchmark for designing future laser-nuclear experiments.

IV. SUMMARY

In summary, we delve into the impact of extreme laser fields on cluster radioactivity from the perspective of nuclear structure information. For different parent nuclei emitting the same cluster, while the rate of change of the penetration probability varies significantly, its overall range exhibits a linear increase with the proton number of the emitted cluster. Furthermore, analysis of various isotope chains reveals that the laser field's influence on the penetration probability is strongly modulated by shell effects and odd-even staggering. Specifically, the neutron shell effect on this change rate gradually weakens as the number of valence protons increases. The association between the change rate of penetration probability and the quadrupole deformation parameter of the parent nucleus is also discussed. The results indicate that the change rate is affected by the degree of nuclear deformation. Finally, for different parent nuclei emitting the same cluster, the relationship between the rate of change of the penetration probability and the decay energy exhibits two distinct inverse correlations with different slopes, further highlighting the role of shell effects. This work can provide a new perspective and deep insights into understanding the interactions between the laser fields and the nuclear decay process.

References

[1] S. A. Giuliani, Z. Matheson, W. Nazarewicz *et al.*, Rev. Mod. Phys. **91**, 011001 (2019)
[2] A. Sandulescu, D. N. Poenaru, and W. Greiner, Sov. J. Part. Nucl. **11**, 06 (1980)
[3] H. J. Rose and G. A. Jones, Nature **307**, 245 (1984)
[4] X. Liu, J. D. Jiang, X. Chen *et al.*, Phys. Rev. C **110**, 034329 (2024)
[5] H. M. Liu, Y. T. Zou, X. Pan *et al.*, Phys. Scr. **96**, 125322 (2021)
[6] C. Qi, F. R. Xu, R. J. Liotta *et al.*, Phys. Rev. Lett. **103**, 072501 (2009)
[7] D. D. Ni, Z. Z. Ren, T. K. Dong *et al.*, Phys. Rev. C **78**, 044310 (2008)
[8] L. J. Qi, D. M. Zhang, S. Luo *et al.*, Phys. Rev. C **108**, 014325 (2023)
[9] L. J. Qi, D. M. Zhang, S. Luo *et al.*, Chin. Phys. C **47**, 014101 (2023)
[10] Z. Z. Ren, C. Xu, and Z. J. Wang, Phys. Rev. C **70**, 034304 (2004)
[11] K. P. Santhosh, R. K. Biju, and A. Joseph, J. Phys. G: Nucl. Part. Phys. **35**, 085102 (2008)
[12] D. N. Poenaru, R. A. Gherghescu, and W. Greiner, Phys. Rev. Lett. **107**, 062503 (2011)
[13] H. F. Zhang, J. M. Dong, G. Royer *et al.*, Phys. Rev. C **80**, 037307 (2009)
[14] J. H. Cheng, W. Y. Zhang, Q. Xiao *et al.*, Phys. Lett. B **848**, 138322 (2024)
[15] K. A. Tanaka, K. M. Spohr, D. L. Balabanski, *et al.*, Matter Radiat. Extrem. **5**, 024402 (2020)
[16] J. W. Yoon, Y. G. Kim, I. W. Choi *et al.*, Optica **8**, 630 (2021)
[17] K. Ueda, Appl. Sci. **8**, 879 (2018)
[18] P. Price, L. Cook, and A. Markert, Nature **325**, 137 (1987)
[19] D. S. Delion, Phys. Rev. C **80**, 024310 (2009)
[20] K. Wei and H. F. Zhang, Phys. Rev. C **102**, 034318 (2020)
[21] K. P. Santhosh, B. Priyanka, and M. S. Unnikrishnan, Nucl. Phys. A **889**, 29 (2012)
[22] K. P. Santhosh and T. A. Jose, Indian J. Phys. **95**, 121 (2021)
[23] M. Ismail, A. Y. Ellithi, M. M. Selim *et al.*, J. Phys. G **47**, 055105 (2020)
[24] M. R. Pahlavani and F. Ahmadvand, Chin. J. Phys **90**, 49 (2024)
[25] D. N. Poenaru, W. Greiner, M. Ivascu *et al.*, Phys. Rev. C **32**, 2198 (1985)
[26] M. Wang, W. J. Huang, F. G. Kondev *et al.*, Chin. Phys. C **45**, 030003 (2021)
[27] F. G. Kondev, M. Wang, W. J. Huang *et al.*, Chin. Phys. C **45**, 030001 (2021)
[28] Z. Wang and Z. Z. Ren, Phys. Rev. C **108**, 024306 (2023)
[29] M. Balasubramaniam and N. S. Rajeswari, Int. J. Mod. Phys. E **23**, 1450018 (2014)
[30] S. Kumar and R. K. Gupta, Phys. Rev. C **55**, 218 (1997)
[31] Y. J. Shi and W. J. Swiatecki, Phys. Rev. Lett. **54**, 300 (1985)
[32] G. Royer, J. Phys. G **26**, 1149 (2000)
[33] M. Ismail, A. Y. Ellithi, M. M. Selim *et al.*, Phys. Scr. **95**, 075303 (2020)
[34] F. Saidi, M. R. Oudih, M. Fellah *et al.*, Mod. Phys. Lett. A **30**, 1550150 (2015)

[35] P. Möller, A. J. Sierk, T. Ichikawa *et al*., At. Data Nucl. Data Tables **109**, 1 (2016)
[36] C. Y. Wong, Phys. Rev. Lett. **31**, 766 (1973)
[37] R. K. Gupta, M. Balasubramaniam, R. Kumar *et al*., J. Phys. G **31**, 631 (2005)
[38] X. Liu, J. D. Jiang, X. J. Wu *et al*., Chin. Phys. C **48**, 054101 (2024)
[39] Ş. Mişicu and M. Rizea, J. Phys. G: Nucl. Part. Phys. **40**, 095101 (2013)
[40] Ş. Mişicu and M. Rizea, J. Phys. G: Nucl. Part. Phys. **46**, 115106 (2019)
[41] J. T. Qi, L. B. Fu, and X. Wang, Phys. Rev. C **102**, 064629 (2020)
[42] X. Liu, J. D. Jiang, L. J. Qi *et al*., Chin. Phys. C **47**, 094103 (2023)
[43] R. Wang, R. Y. Wang, Y. B. Qian *et al*., Chin. Phys. C **41**, 064103 (2017)
[44] H. M. Elsharkawy and M. Saleh Yousef, Nucl. Phys. A **959**, 1 (2017)
[45] L. J. Liao, Y. Fan, X. Liu *et al*., Phys. Rev. C **112**, 014327 (2025)